International Journal of Neural Systems, Vol. 17, No. 4 (2007) 319–327

World Scientific
www.worldscientific.com

DOES ABNORMAL SPINAL RECIPROCAL INHIBITION LEAD TO CO-CONTRACTION OF ANTAGONIST MOTOR UNITS? A MODELING STUDY

VASSILIS CUTSURIDIS
Department of Computing Science and Mathematics,
University of Stirling, Stirling FK9 4LA, Scotland
vcu@cs.stir.ac.uk

It is suggested that co-contraction of antagonist motor units perhaps due to abnormal disynaptic I_a reciprocal inhibition is responsible for Parkinsonian rigidity. A neural model of Parkinson's disease bradykinesia is extended to incorporate the effects of spindle feedback on key cortical cells and examine the effects of dopamine depletion on spinal activities. Simulation results show that although reciprocal inhibition is reduced in DA depleted case, it doesn't lead to co-contraction of antagonist motor neurons. Implications to Parkinsonian rigidity are discussed.

Keywords: Parkinson's disease; dopamine; reciprocal inhibition; spinal cord; rigidity; neural model.

1. Introduction

Parkinson's disease (PD) is associated with a wealth of motor impairments such as resting tremor, akinesia, rigidity, bradykinesia and impaired postural reflexes. Bradykinesia is the hallmark and most disabling symptom of PD. Recently, a neural model of PD bradykinesia was advanced by Cutsuridis and Perantonis.[1,2] The model was successful at offering an alternative explanation to what other models[24] have suggested about the causes of Parkinson's disease bradykinesia. More specifically, it focused more on the effects of dopamine (DA) depletion in cortex and spinal cord and less on its effects in basal ganglia (BG) (as other models have done). The model provided a unified theoretical framework for PD bradykinesia and it was capable of producing a wealth of neuronal, electromyographic (EMG) and behavioral movement empirical findings such as:

- Increased cellular reaction time
- Prolonged behavior reaction time
- Increased duration of neuronal discharge in area 4 preceding and following onset of movement
- Reduction of firing intensity and firing rate of cells in primary motor cortex
- Abnormal oscillatory globus pallidus internal segment (GPi) response
- Disinhibition of reciprocally tuned cells
- Increases in baseline activity
- Repetitive bursts of muscle activation
- Prolongation of premotor and electromechanical delay times
- Reduction in the size and rate of development of the first agonist burst of EMG activity
- Asymmetric increase in the time-to-peak and deceleration time
- Decrease in the peak value of the velocity trace
- Increase in movement duration
- Substantial reduction in the size and rate of development of muscle production
- Movement variability

The present work extends this model in two ways: (1) It incorporates the spindle feedback not only in the spinal cord as in,[1,2] but also in cortex and examines its effects on the activities of specific types of cells found in primary motor cortex both in normal and in DA depleted cases, and (2) it examines the effects of DA depletion not only in alpha motoneuronal (MN) and Renshaw activities as in Ref. 1, but also in the activities of type I_a and I_b

inhibitory interneurons (IN) and primary spindles. Abnormal reciprocal inhibition has been suggested to play a significant role in PD rigidity.[6,7] More specifically, reduced reciprocal inhibition of I_aINs disinhibit antagonist aMNs and thus lead to co-contraction of antagonist muscles in parkinsonian patients[25] and in MPTP treated monkeys.[11] Preliminary simulation results will show that although reciprocal inhibition is reduced in DA depleted case as it has been reported in the literature,[6,7] it doesn't lead to co-contraction of antagonist aMNs.[11]

2. Methods

2.1. *Mathematical formalism*

Figure 1 schematizes the components of the DA innervated cortico-spinal network with cortical spindle feedback. The present network extends the model of Cutsuridis and Perantonis[1,2] for single joint ballistic arm movements in Parkinson's disease bradykinesia by studying the effects of the spindle feedback on the activities of reciprocal and bidirectional neurons in area 4. The effects of DA depletion on the activities of spinal elements such as I_a inhibitory interneurons (IN), Renshaw cells and alpha motorneurones (MN) are also examined. Table 1 depicts the correspondence of the cortical model and brain elements. Evidence for the connectivity and physiology of the model's elements can be found in Table 2 of Refs. 3 and 5. Evidence for DA innervation of primate neocortex and spinal cord can be found in Refs. 1, 12–19, 22–23.

Most of the equations (Eqs. (1), (3)–(12), (14), (20), (22)–(23)) presented in this section have been developed before by other researchers.[1–5] Eq. (2) has been altered from Ref. 1 to incorporate the effects of spindle feedback on cortical neuronal activities, whereas new equations are also introduced (see Eqs. (13), (15)–(19), (21)). In this section we list all equations (new and old) in order to enhance the readability of the paper and help its readers.

In the model, the output of the BG system, which represents the activity of the GPi is modeled by the GO signal

$$G(t) = G_0(t - \Im_i)^2 u[t - \Im_i]/(\beta + \gamma(t - \Im_i)^2) \quad (1)$$

where G_0 amplifies the GO signal, $\Im_i$ is the onset time of the ith volitional command, β and γ are free parameters, and $u[t]$ is a step function that jumps

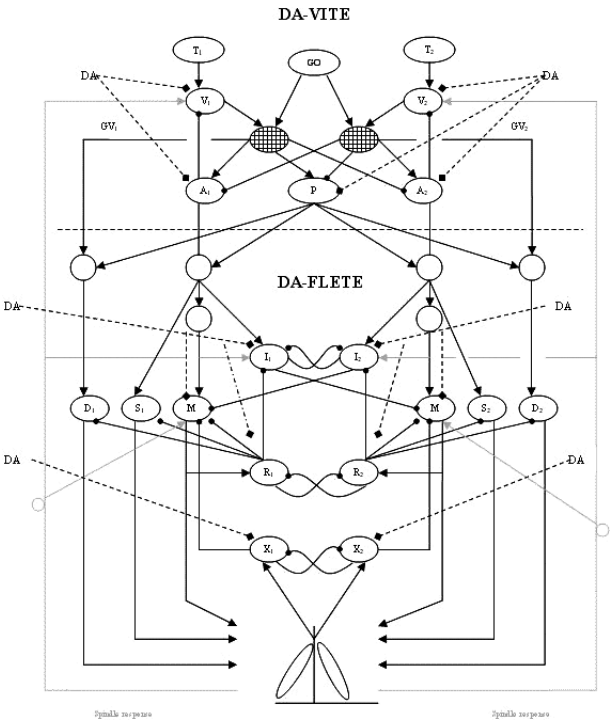

Fig. 1. Neural architecture of the proposed dopamine modulated cortico-spinal model with muscle spindle feedback to cortex. (Top) The DA-VITE model for trajectory generation. (Bottom) The DA-FLETE model of the opponent processing spinomuscular system. Arrow lines, excitatory projections; solid-dot lines, inhibitory projections; diamond dashed lines, dopamine modulation; gray arrow lines, excitatory spindle feedback projections. Note in this model the spindle response projects not only to spinal cord, but also to the cortex (area 5 difference vector (DV)). DA, dopamine modulatory signal; GO, basal ganglia output signal; P, bi-directional co-contractive signal; T, target position command; V_i, difference vector (DV) activity; GV_i, desired velocity activity; A, current position command; M, alpha motorneuronal (MN) activity; R, Renshaw cell activity; I, type I_a spinal IN; X, type I_b spinal IN; S, gamma static MN activity; D, gamma dynamic MN activity; 1, 2, antagonist cell pair.

from 0 to 1 to initiate movement. The difference vector (DV), is described by

$$\frac{dV_i}{dt} = 30(-V_i + T_i - DA_1 \cdot A_i + DA_1 \cdot a_w \cdot (W_i(t-\tau) - W_j(t-\tau)) \quad (2)$$

where T_i is the target position command, A_i is the current limb position command, a_w is the gain of spindle feedback and DA_1 is the modulatory effect of dopamine on area 4's PPV inputs to DV cell activity. Dopamine's values can range from 0 (lesioned) to 1 (normal). The desired velocity vector (DVV),

Table 1. Correspondence between cortical model and brain elements.

Model element	Brain element	Reference
Desired velocity vector (DVV)	Area 4 reciprocal cell activity	10
Co-contractive vector (P)	Area 4 bidirectional cell activity	10
Present position vector (PPV)	Area 4 tonic cell activity	3 and references therein
Difference vector (DV)	Area 5 phasic cell activity	3 and references therein
Target position vector (TPV)	Area 5	3 and references therein
GO signal	Globus pallidus internal segment	3 and references therein

which represents area's 4 reciprocally activated cell activity,[10] is defined by

$$u_i = [G \cdot (DA_2 \cdot V_i - DA_3 \cdot V_j) + B_u/DA_4]^+ \quad (3)$$

where i, j designate opponent neural commands, B_u is the baseline activity of the phasic-MT area 4 cell activity, and DA_2, DA_3, are the modulatory effects of dopamine on DV inputs to DVV cell activity and DA_4 is the effect of dopamine on DVV baseline activity. The reader should refer to Ref. 1 for detailed explanations as to why the DV flexion (V_i) cell is modulated by a different DA parameter (DA_2) from the DV extension (V_j) cell (DA_3).

The co-contractive vector (P), which is represented by area's 4 bidirectional neuronal activity[10] is given by

$$P = [G \cdot (DA_2 \cdot V_i - DA_3 \cdot V_j) + B_P/DA_4]^+ \quad (4)$$

The present position vector (PPV) dynamics is defined by

$$\frac{dA_i}{dt} = G[DA_2 \cdot V_i]^+ - G[DA_3 \cdot V_j]^+ \quad (5)$$

The quadratic force-length relationship of muscle is approximated by

$$F_i = k([L_i - \Gamma_i + C_i]^+)^2 \quad (6)$$

where k is a scaling parameter, F_i is muscle force, L_i is muscle length, Γ_i is resting muscle length, C_i is muscle contractile state and indices $i = \{1, 2\}$ designate antagonist muscle pairs. The contractile state dynamics is defined by

$$\frac{dC_i}{dt} = \beta_i[(B_i - C_i)M_i - C_i] - [F_i - \Gamma_F]^+ \quad (7)$$

where Γ_F is the force threshold, M_i is the alpha-motoneuron (α-MN) pool activity in muscle control channel i, β_i is the contractile rate, and B_i is the number of contractile fibers recruited. The muscle lengths for opponent biceps (BIC) and triceps (TRI) muscles are

$$L_1 = \sqrt{((20 - \sin(\Theta))^2 + (\cos(\Theta)^2)} \quad (8)$$

and

$$L_2 = \sqrt{((20 + \sin(\Theta))^2 + (a\cos(\Theta))^2)} \quad (9)$$

where L_1 and L_2 are the lengths of the BIC and TRI muscles and Θ is the angle of rotation. The limb dynamics is defined by

$$\frac{d^2\Theta}{dt^2} = \left(F_1 - F_2 + F_e - \eta\frac{d\Theta}{dt}\right) \Big/ I_m \quad (10)$$

where F_e is the external force, η is the viscosity and I_m is the moment of inertia. The contraction rate is defined by

$$\beta_i = 0.05 + 0.01(A_i + P + E_i) \quad (11)$$

where A_i is the descending present position command, P is the coactivation signal, and E_i is the stretch feedback from the spindles. Likewise, the number of contractile fibers recruited into force are:

$$B_i = 0.05 + 0.01(A_i + P + E_i) \quad (12)$$

Renshaw population cell activity is modeled by

$$\frac{dR_i}{dt} = \phi(\lambda B_i - R_i)DA_5 z_i \max(M_i, 0) - DA_6 \cdot R_i(1.5 + \max(R_j, 0)) \quad (13)$$

where the Renshaw cell recruitment rate z_i is:

$$z_i = 0.02(1 + \max(M_i, 0)) \quad (14)$$

and it depends on the level of α-MN activation. The α-MN population activity is described by the following equation

$$\frac{dM_i}{dt} = \phi(\lambda B_i - M_i) \cdot DA_7 \cdot (A_i + P + \chi \cdot E_i) - (M_i + 2) \cdot DA_8 \cdot (1 + \Omega \cdot \max(R_i, 0) + \rho \cdot \max(X_i, 0) + \max(I_j 0)) \quad (15)$$

where X_i is the type I_b interneuron (I_bIN) force feedback and I_j is the type I_a interneuron. The type

I_a interneuron (I_aIN) population activity is defined as

$$\frac{dI_i}{dt} = \phi \cdot (15 - I_i) \cdot DA_9 \cdot (A_i + P + \chi E_i) - DA_{10} \cdot I_i(1 + \Omega \cdot \max(R_i, 0) + \max(I_j^{\cdot}0)) \quad (16)$$

The I_bIN population activity is excited by feedback activity of force-sensitive Golgi tendon organs

$$\frac{dX_i}{dt} = \phi \cdot DA_{11}(15 - X_i)F_i - X_i \cdot DA_{11} \cdot (0.8 + 2.2\max(X_j, 0)) \quad (17)$$

The static γ-MN activity is described by

$$\frac{dS_i}{dt} = \phi(10 - S_i)(A_i + P) - S_i[1.8 + 0.2h(R_i)] \quad (18)$$

where $h(w) = \max(w, 0)/(0.3 + \max(w, 0))$. The intrafusal muscle contraction associated with static γ-MN activation is described by

$$\frac{dU_i}{dt} = 4S_i - U_i \quad (19)$$

The dynamic γ-MN activity is

$$\frac{dD_i}{dt} = (8 - D_i)(100G[V_i]^+ + P) - (D_i + 1.2)(1 + 100G[V_j]^+ + 0.5h(R_i)) \quad (20)$$

The intrafusal muscle contraction associated with dynamic γ-MN activation is

$$\frac{dN_i}{dt} = 4D_i - 6N_i \quad (21)$$

The spindle receptor activation was defined as

$$\frac{dW_i}{dt} = (2 - W_i)(G_s \cdot [U_i + L_i - \Gamma_i]^+) + G_v\left(\left[N_i + \frac{dL_i}{dt}\right]^+\right)^{0.3} - 10W_i \quad (22)$$

The stretch feedback signal is given by

$$E_i = a_e \cdot W_i \quad (23)$$

where a_e is the feedback gain signal.

2.2. *Implementation details*

The simulations were performed on a Pentium IV 1.7 GHz PC with MATLAB's version R2006b installed. The whole system of differential and algebraic equations was implemented in MATLAB (The MathWorks, Inc, Natick, MA). Differential equations were integrated numerically using one of the MATLAB ordinary differential equation solvers (mainly ode45), an implicit solver based on the Dormand-Prince pair method.[9] Relative (error) tolerance was set to 10^{-6}. The parameters for the normally functioning and DA depleted basal ganglio-cortico-spinal network used in the simulations are depicted in Table 2.

3. Simulation Results

3.1. *Effects of spindle feedback on area's 4 neuronal activities*

Figure 2 depicts a qualitative comparison of cortical neuronal peristimulus time histograms (PSTH)[10] (columns 1 and 3) and simulated cell responses (columns 2 and 4) in area 4 for flexion, extension and co-contraction of a normal monkey during a simple voluntary reaching task. Briefly in Ref. 10, normal and MPTP-treated monkeys were trained to make fast ballistic flexion and extension movements of the forearm, while their cortical activities were recorded. They reported the existence of three types of cells in area 4: (1) reciprocally activated (RO) cells, (2) bidirectionally activated (BD) cells, which are activated for both direction of movement and (3) unidirectional (UD) cells, which are activated for only one direction of movement. Details concerning the functional roles of these types of cells in the generation of movement can be found in Ref. 1. A clear tri-phasic AG_1-ANT-AG_2 reciprocal pattern of cellular activity is reported (column 1 of Fig. 2). Similarly, the activity of bidirectional neurons tuned to both directions of movement is also shown (column 3 of Fig. 2). The model is able to simulate successfully the activities of both reciprocal (DVV activity) cellular activity and bidirectional neurons (co-contractive vector, P) (columns 2 and 4 of Fig. 2). The simulated marked by an arrow first peak of extension and second peak of flexion reciprocal cells is primarily due to spindle feedback input to DV activity (a feature lacking in Ref. 1).

Figure 3 shows qualitative comparisons of experimentally derived and simulated reciprocally (columns 1 and 2, respectively) and bidirectionally (columns 3 and 4, respectively) activated neurons. The simulated cell responses were produced when the output of the basal ganglia was reduced and the cortical and spinal dopamine was depleted (see Table 2 for parameter values). Clearly the tri-phasic pattern is disrupted: AG_1 and AG_2 have merged and

Table 2. Model parameter values in normal and DA depleted cases.

Symbol	Value		Symbol	Value	
	Normal	DA depleted		Normal	DA depleted
g_0	0.095	0.075	ρ	1	1
k	1	1	Ω	1	1
η	0.4	0.4	τ	5	5
I_m	1	1	F_e	0	0
λ	5	5	DA_1	1	0.99
T_1	0.75	0.75	DA_2	1	0.9
T_2	0.3	0.3	DA_3	1	0.8
G_1	21.01	21.01	DA_4	1	0.8
G_2	21.01	21.01	DA_5	1	0.8
G_v	1	1	DA_6	1	0.8
G_s	1	1	DA_7	1	0.8
G_f	1	1	DA_8	1	0.9
β	25.5	55.5	DA_9	1	0.8
γ	1	1	DA_{10}	1	0.9
δ	1	1	τ_2	20	20
ϕ	0.1	0.1	B_u	0.02	0.02
a_w	0.06	0.06	DA_{11}	1	0.9
χ	1	1	B_p	0.05	0.05

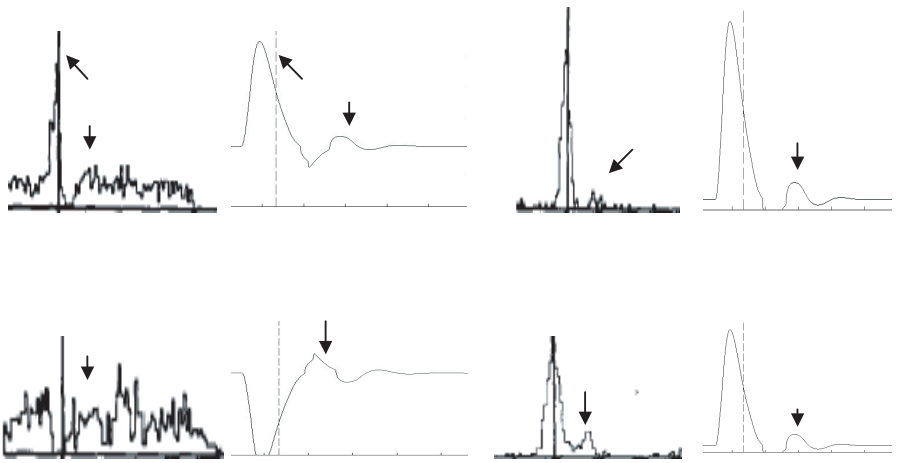

Fig. 2. Comparison of peristimulus time histograms (PSTH) of reciprocally organized neurons (column 1; reproduced with permission from Ref. 10, Fig. 4A, p.182, Copyright © Springer-Verlag) in area 4, simulated area's 4 reciprocally organized phasic (DVV) cell activities (column 2), PSTH of area's 4 bidirectional neurons (column 3; reproduced with permission from Ref. 10, Fig. 4A, p.182, Copyright © Springer-Verlag) and simulated area's 4 co-contractive (P) cells activities (column 4) for a flexion (A and C) and extension (B and D) movements in abnormal monkey. The vertical bars indicate the onset of movement. Note a clear tri-phasic AG_1-ANT-AG_2 pattern marked with arrows is evident in PSTH of reciprocally organized neurons. The same tri-phasic pattern is evident in simulated DVV cell activities. The second peak in simulated activities marked with an arrow arises from the spindle feedback input to area's 5 DV activity.

ANT burst is considerably shortened. In addition, the same DA depleted effects as the ones reported in Ref. 1 are evident, that is there is an overall reduction of firing intensity[10,27] (0.0175 in normal case, 0.008 in DA depleted case), a reduced rate of change of neuronal discharge,[10,27] a disorganization of neuronal activity (neuronal direction specificity is reduced),[10] an increase in baseline activity[10,27] (0.05 in normal case, 0.065 in DA depleted case) and an increased duration in neuron discharge in

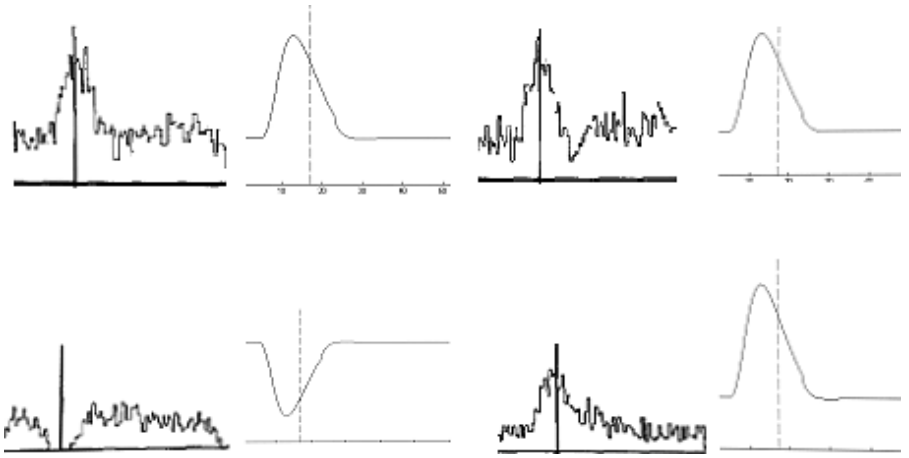

Fig. 3. Comparison of peristimulus time histograms (PSTH) of reciprocally organized neurons (column 1; reproduced with permission from Ref. 10, Fig. 4B, p.182, Copyright © Springer-Verlag) in area 4, simulated area's 4 reciprocally organized phasic (DVV) cell activities (column 2), PSTH of area's 4 bidirectional neurons (column 3; reproduced with permission from Ref. 10, Fig. 4B, p.182, Copyright © Springer-Verlag) and simulated area's 4 co-contractive (P) cells activities (column 4) for a flexion (A and C) and extension (B and D) movements in an MPTP-treated monkey. The vertical bars indicate the onset of movement. Note that the tri-phasic pattern is disrupted: AG_1 and AG_2 have merged, and ANT pause is shortened.

area 4 preceding and following onset of movement resulting in a prolongation of its total response duration, exactly as it has been observed in experimental studies[10,11,26,27] (11.23 in normal case, 13.46 in DA depleted case).

3.2. *Effects of dopamine depletion on spinal activities*

Fast goal-directed voluntary movements are known to be associated with three distinct bursts of EMG activity in antagonist muscles. The first agonist burst provides the impulse force for the movement, whereas the antagonist activity provides the braking force to halt the limb. Sometimes a second burst is needed to bring the limb to the final position. In PD patients movements up to a certain size might be performed relatively normally,[29] but there are times that movements would require additional bursts of EMG activity due to inappropriate scaling of the first agonist burst.[30] A plausible hypothesis of why PD EMG agonist burst activity is reduced and why sometimes multiple bursts of AG-ANT-AG are needed to complete the movement has been presented in Refs. 1, 2.

Figure 4 shows qualitative simulations of alpha MNs and type I_aINs in normal (column 1) and DA depleted (column 2) cases. A triphasic pattern of neuronal activation marked by arrows (column 1) is evident at both the aMN and I_a levels. In DA depleted case (column 2) the temporal sequence of EMG bursts (AG-ANT-AG) is preserved, but disrupted: AG_1 and ANT are shortened, whereas AG_2 at the aMN level is completely abolished. Also, the background cell activity of aMNs is increased. The intensities of both aMNs and I_a activities and their rates of change are reduced (EMGmax is 3.62 in normal case and 3.18 in DA depleted case), whereas the duration of their discharge before and after onset of movement is increased. An interesting simulation result is that although the disynaptic I_a reciprocal inhibition is reduced[6,7] and hence there is disinhibition of antagonist MNs, there is no co-contraction of antagonist motor units (see column 2 of Fig. 4) as it has been reported in experimental studies.[11,25,28] There is, however, a disorganization of neuronal spinal activity (that is cells that were pausing their activities before DA depletion the same cells are activated in post DA depletion (see marked region in column 2 of Fig. 4)) similar to the one in cortex.

For this particular simulation movement (final target position: 0.76 rad or 44° in normal case), the simulated PD patient undershoots the target (final target position: 0.59 or 33°). An additional biphasic pattern of muscle activation is required in order for

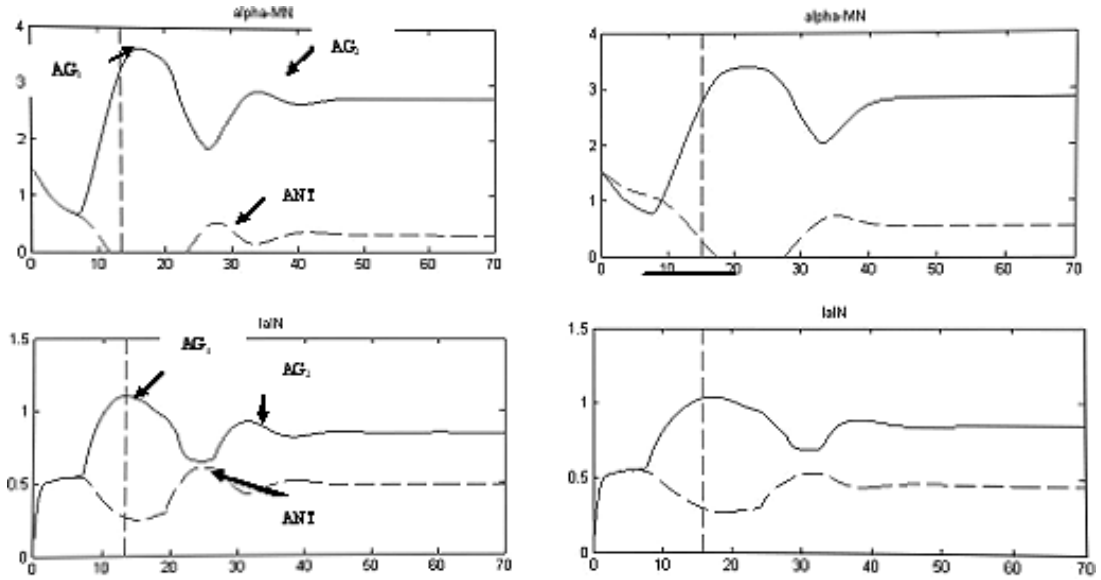

Fig. 4. Comparison of simulated reciprocal alpha motoneuronal (MN) and type Ia inhibitory interneuron (IN) activities in normal (column 1) and DA depleted (column 2) cases. Note a clear tri-phasic pattern of activation marked by arrows at the levels of αMNs and I_aIns (column 1). The same pattern is disrupted in DA depleted case (column 2; see text for which features are disrupted). The vertical bars indicate the onset of movement.

the limb to reach the target position (not shown, but see Refs. 1, 2).

4. Discussion

The present model is an extension of the Cutsuridis and Parantonis[1] neural model of voluntary movement and proprioception in Parkinson's disease bradykinesia. Although the latter model was successful in its regard in simulating a wealth of neuronal, EMG and kinematic data from PD patients and MPTP-treated animals, it was extended by the former model to incorporate experimental evidence regarding the effects of spindle feedback on cortical cell activities as well as examine the effects of DA depletion on spinal activities, particularly the reciprocal disynaptic I_a inhibition and its effects on the activities of reciprocally activated α MNs.

The present model is successful at simulating accurately the neuronal activities of two types of cells found in primary motor cortex,[10] that is the activities of the reciprocal and bidirectional cells. The model predicted that the triphasic pattern of neuronal activation[10] at the level of area 4 DVV activity, clearly evident in Fig. 2, is due to the spindle feedback input to posterior parietal neuronal activities.[5,31] This triphasic pattern then drives the antagonist α MNs and contributes to the generation of the triphasic pattern of muscle activation responsible for bringing the limb from an initial to a final position. In Ref. 1 these two types of cells represented two separate movement control systems found to exist experimentally[32]: the activity of reciprocal neurons was organized for the reciprocal activation of antagonist muscles, whereas the activity of bidirectional neurons was organized for the co-contraction of antagonist muscles. Whereas the reciprocal pattern of muscle activation served to move the joint from an initial to a final position, the antagonist co-contraction served to increase the apparent mechanical stiffness of the joint, thus fixing its posture or stabilizing its course of movement in the presence of external force perturbations.

An interesting simulation result of the model was that the reduced reciprocal disynaptic Ia inhibition[6–8] in the DA depleted case doesn't lead to the co-contraction of antagonist motor units.[8,11,20,21,25] The co-contraction of reciprocally activated MNs has been suggested as a potential mechanism for Parkinson's disease rigidity.[7] The model predicts that although the co-contraction of antagonist muscles might be a mechanism for PD rigidity, the co-contraction isn't due to abnormal

reciprocal inhibition at the spinal level. The causes of MN co-contraction outght to be searched more centrally, potentially in the microcircuit of the motor cortex and/or the basal ganglia.[7] Future extensions of the present model will address this finding by introducing a detailed basal ganglio-cortico laminar model that will account for all known anatomical, neurochemical and neurophysiological evidence of these structures and examine in a more quantitative way the effects of DA depletion on their neuronal activities.

References

1. V. Cutsuridis and S. Perantonis, A neural network model of Parkinson's Disease Bradykinesia, *Neural Networks* **19** (2006) 354–374.
2. V. Cutsuridis, Neural model of dopaminergic control of arm movements in Parkinson's Disease Bradykinesia, in *Artificial Neural Networks: Cognitive Machines — ICANN '06*, *Lecture Notes in Computer Science*, LNCS 4131 (Springer-Verlag, Berlin) (2006), pp. 583–591.
3. J. L. Contreras-Vidal, S. Grossberg and D. Bullock, A neural model of cerebellar learning for arm movement control: Cortico-spino-cerebellar dynamics, *Learn. Mem.* **3**(6) (1997) 475–502.
4. D. Bullock and S. Grossberg, Adaptive neural networks for control of movement trajectories invariant under speed and force rescaling, *Human Movement Science* **10** (1991) 3–53.
5. D. Bullock, P. Cisek and S. Grossberg, Cortical networks for control of voluntary arm movements under variable force conditions, *Cerebral Cortex* **8** (1998) 48–62.
6. S. Meunier, S. Pol, J. L. Houeto and M. Vilailhet, Abnormal reciprocal inhibition between antagonist muscles in Parkinson's disease, *Brain* **123** (2000) 1017–1026.
7. S. Lelli, M. Panizza and M. Hallett, Spinal cord inhibitory mechanisms in Parkinson's disease, *Neurology* **41** (1991) 553–556.
8. A. Berardelli, A. F. Sabra and M. Hallett, Physiological mechanisms of rigidity in Parkinson's disease, *J. Neurol. Neurosurg. Psychiatry* **46** (1983) 45–53.
9. J. R. Dormand and P. J. Prince, A family of embedded Runge-Kutta formulae, *J. Comp. Appl. Math.* **6** (1980) 19–26.
10. D. J. Doudet, C. Gross, M. Arluison and B. Bioulac, Modifications of precentral cortex discharge and EMG activity in monkeys with MPTP induced lesions of DA nigral lesions, *Exp. Brain Res.* **80** (1990) 177–188.
11. A. Benazzouz, C. Gross, J. Dupont and B. Bioulac, MPTP induced hemiparkinsonism in monkeys: Behavioral, mechanographic, electromyographic and immunohistochemical studies, *Exp. Brain Res.* **90** (1992) 116–120.
12. B. Berger, S. Trottier, C. Verney, P. Gaspar and C. Alvarez, Regional and laminar distribution of dopamine and serotonin innervation in the macaque cerebral cortex: A radioautographic study, *J. Comp. Neurol.* **273** (1988) 99–119.
13. A. Bjorklund and G. Skagerberg, Evidence of a major spinal cord projection from the diencephalic A11 dopamine cell group in the rat using transmitter-specific fluoroscence retrograde tracing, *Brain Res.* **177** (1979) 170–175.
14. W. W. Blessing and J. P. Chalmers, Direct projection of catecholamine (presumably dopamine)-containing neurons from the hypothalamus to spinal cord, *Neurosci. Lett.* **11** (1979) 35–40.
15. J. W. Commissiong, S. Gentleman and N. H. Neff, Spinal cord dopaminergic neurons: Evidence for an uncrossed nigrostriatal pathway, *Neuropharmacology* **18** (1979) 565–568.
16. P. Gaspar, I. Stepniewska and J. H. Kaas, Topography and collateralization of the dopaminergic projections to motor and lateral prefrontal cortex in owl monkeys, *J. Comp. Neurol.* **325** (1992) 1–21.
17. P. Gaspar, C. Duyckaerts, C. Alvarez, F. Javoy-Agid and B. Berger, Alterations of dopaminergic and noradrenergic innervations in motor cortex in Parkinson's disease, *Ann. Neurol.* **30** (1991) 365–374.
18. A. Dubois, M. Savasta, O. Curet and B. Scatton, Autoradiographic distribution of the D_1 agonist [$_3$H]SKF 38393, in the rat brain and spinal cord. Comparison with the distribution of D_2 dopamine receptors, *Neuroscience* **19** (1986) 125–137.
19. J. D. Elsworth, A. Y. Deutch, D. E. Redmond, J. R. Sladek and R. H. Roth, MPTP reduces dopamine and norepinephrine concentrations in the supplementary motor area and cingulate cortex of the primate, *Neuroscience Letters* **114** (1990) 316–322.
20. P. J. Delwaide and J. L. Pepin, A. Maertens de Noordhout, Short-latency autogenic inhibition in patients with parkinsonian rigidity, *Ann. Neurol.* **30** (1991) 83–89.
21. J. Jankovic, Pathophysiology and clinical assessment of motor symptoms in Parkinson's disease, in *Handbook of Parkinson's disease*, WC Koller (ed.) (1987).
22. D. A. Lewis, J. H. Morrison and M. Goldstein, Brainstem dopaminergic neurons project to monkey parietal cortex, *Neuroscience Letters* **86** (1988) 11–16.
23. M. S. Lidow, P. S. Goldman-Rakic, D. W. Gallager, D. H. Geschwind and P. Rakic, Distribution of major neurotransmitter receptors in the motor and somatosensory cortex of the rhesus monkey, *Neuroscience* **32**(3) (1989) 609–627.
24. J. L. Contreras-Vidal and G. Stelmach, A neural model of basal ganglia-thalamocortical relations in normal and parkinsonian movement, *Biol. Cybernetics* **73** (1995) 467–476.

25. C. Ohye, N. Tsukahara and H. Narabayashi, Rigidity and disturbance of reciprocal innervation, *Confin. Neurol.* **26** (1965) 24–40.
26. R. L. Watts and A. S. Mandir, The role of motor cortex in the pathophysiology of voluntary movement deficits associated with parkinsonism, *Neurol. Clin.* **10**(2) (1992) 451–469.
27. C. Gross, J. Feger, J. Seal, P. Haramburu and B. Bioulac, Neuronal activity of area 4 and movement parameters recorded in trained monkeys after unilateral lesion of the substantia nigra, *Exp. Brain Res.* Suppl. **7** (1983) 181–193.
28. K. D. Phann, A. S. Buchman, C. L. Comella and D. M. Corcos, Control of movement distance in Parkinson's disease, *Mov Disord* **16**(6) (2001) 1048–1065.
29. K. A. Flowers, Visual "closed-loop" and "open-loop" characteristics of voluntary movement in patients with Parkinsonism and intention tremor, *Brain* **99**(2) (1976) 269–310.
30. M. Hallett and S. Khoshbin, A physiological mechanism of bradykinesia, *Brain* **103** (1980) 301–314.
31. E. G. Jones, J. D. Coulter and H. C. Hendry, Intracortical connectivity of achitectonic fields in the somatic sensory, motor and parietal cortex of monkeys, *J. Comp. Neurol.* **181** (1978) 291–348.
32. D. R. Humphrey and D. J. Reed, Seperate cortical systems for control of joint movement and joint stiffness: Reciprocal activations and coactivation of antagonist muscles, in *Motor control mechanisms in health and disease* (J. E. Desmedt (ed.) New York: New York Raven Press), (1983), pp. 347–372.